

FEDERAL UNIVERSITY OF SANTA CATARINA - ARARANGUÁ

BRUNO ROCHA COLONETTI

FINAL PROJECT

ARARANGUÁ

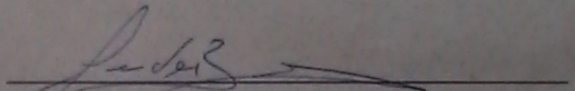
2016

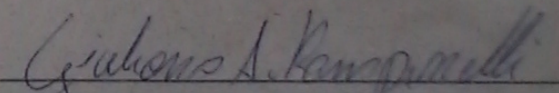
BRUNO ROCHA COLONETTI

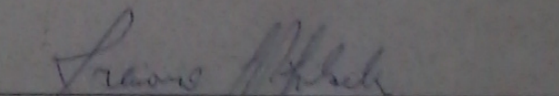
TRABALHO DE CONCLUSÃO DE CURSO DE GRADUAÇÃO EM
ENGENHARIA DE ENERGIA

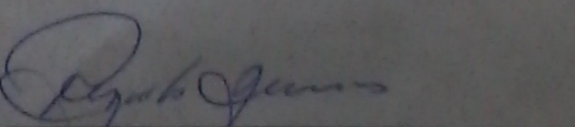
Trabalho de conclusão de curso na modalidade de artigo científico para a aprovação na disciplina de Trabalho de Conclusão de Curso do curso de Engenharia de Energia da Universidade Federal de Santa Catarina – Campus Araranguá

Aprovado em: 08/07/2016


Prof. Leonardo Elizeire Bremermann (Orientador)


Prof. Giuliano Arns Rampinelli (Examinador)


Prof. Luciano Lopes Pflischer (Examinador)


Prof. Reginaldo Geremias (Supervisor)

MODEL FOR THE IMPACT EVALUATION OF ELECTRIC VEHICLE INTEGRATION ON THE ADEQUACY OF GENERATING SYSTEMS

Bruno Rocha Colonetti¹

ABSTRACT

In recent years, the integration of electric vehicles (EVs) into power systems has gained substantial attention by the academia and utilities mainly due to the new opportunities of ancillary services that this technology can offer to power systems. Moreover, the growing presence of renewable energy sources in power systems has brought additional uncertainty to the forecast of available generating capacity. Thereby, this study aims at developing an EV model for evaluating the impact of large-scale EV integration on the adequacy of generating systems. In order to account for the growing presence of wind generation, the proposed method is used to evaluate the impact of EV integration on a modified version of the IEEE RTS - 96 electric system. The results show that large-scale EV integration impact on the adequacy of generating systems depends on the criterion used by EV's owners when deciding whether to recharge their EVs or not. Also, it is shown that the EV impact can be reduced and even be positive, if the EVs are regarded as providers of ancillary services to the grid.

Keywords: Adequacy. Electric vehicle. Generating system. Power systems.

1 INTRODUCTION

In recent years, electric vehicle (EV) technology has gained increasing attention due to its benefits as an environmentally friendly technology. EV sales are expected to increase worldwide in the coming years as EVs become more popular and affordable.

However, EV technology is also a source of concern when its large-scale integration into power systems is taken into consideration. This integration will bring more uncertainty to load forecast and may cause an increase in the peak load, which would require investments in infrastructure to happen sooner than expected.

Furthermore, system operators must cope with the growing presence of renewable energy sources into the generating systems, which brings long and short-term uncertainties to the generation capacity available to meet the system demand.

Hence, this study aims at evaluating the impact of large-scale EV integration on the adequacy of a generating system with high penetration of wind power.

2 BACKGROUND AND STATE-OF-THE-ART

The following sections present the state-of-the-art of the subjects of this study.

2.1 Electric vehicles technology

Electric vehicles (EVs) can be categorized based on the vehicle hybridization rate. Today, there are three main types of EVs (Yong et al., 2015):

- Hybrid electric vehicles (HEVs);
- Plug-in hybrid electric vehicles (PHEVs);
- Battery electric vehicles (BEV).

The next subsections give the characteristics of each EV type.

¹Undergraduate student of Energy Engineering at the Federal University of Santa Catarina, Araranguá Campus, Rodovia Governador Jorge Lacerda, 3201, Jardim das Avenidas, Araranguá, Santa Catarina, Brasil, CEP 88900-000. E-mail: colonettib@gmail.com

2.1.1 Hybrid electric vehicles (HEVs)

The HEVs propel through a combination of internal combustion engine and an electric motor. HEVs generally have a low capacity battery, which is charged by a system of regenerative braking or by the internal combustion engine. These EVs cannot be recharged from the distribution grid (Yong et al., 2015).

Figures 1, 2 and 3 show the most common configurations of an internal combustion engine and an electric motor in a HEV.

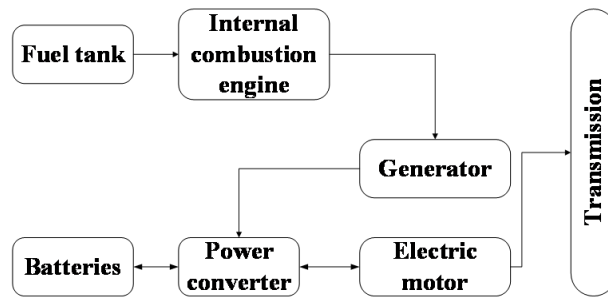


Figure 1: Series HEV

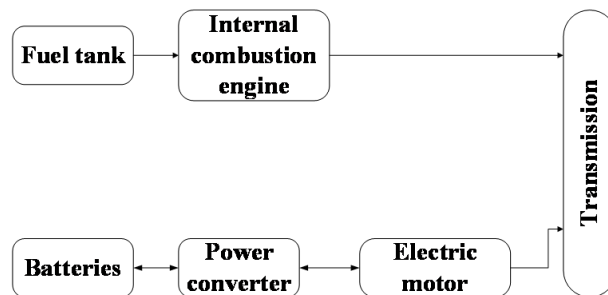


Figure 2: Parallel HEV

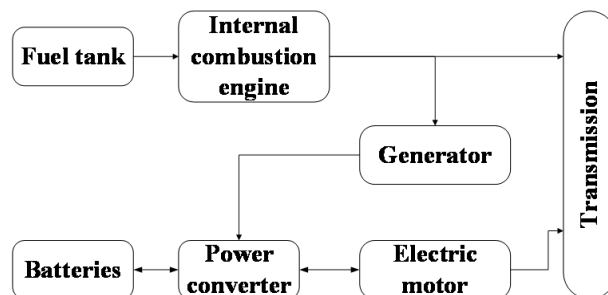


Figure 3: Series-parallel HEV

In a series HEV, figure 1, the transmission is only coupled to the electric motor. The battery of this type of HEV is connected to a generator which in turn is connected to the internal combustion engine. The generator recharges the battery whenever the state-of-charge (SOC) is low. Similarly, the battery is also connected to a regenerative braking system (Yong et al., 2015).

This HEV configuration has the lowest overall efficiency among EVs, it is about 25%. However, series HEVs are suitable for stop-and-run driving patterns, such as in urban perimeters (Tie and Tan, 2013).

As shown in figure 2, in a parallel HEV, the internal combustion engine and the electric motor are mechanically coupled to the transmission and simultaneously transmit power to turn the wheels (Yong et al., 2015).

This HEV configuration is ideal under both highway-driving and city-driving conditions and its overall efficiency is about 43% (Tie and Tan, 2013).

The series-parallel HEV, figure 3, has its internal combustion engine coupled to both the transmission and a generator. Moreover, the electric motor is also connected to the transmission. Thus, this HEV can run either as a series HEV or a parallel HEV. Despite having the benefits of a series HEV and a parallel HEV, a series-parallel HEV has a complicated design and is more costly than the first two HEVs (Yong et al., 2015).

2.1.2 Plug-in hybrid electric vehicles (PHEVs)

As the HEVs, the PHEVs have an internal combustion engine and an electric motor. However, a PHEV can recharge its battery pack with energy from the distribution grid. Additionally, the PHEVs' batteries are larger than the HEVs' what gives the PHEVs a longer all-electric range (Yong et al., 2015).

Similar to the HEVs, the most common PHEVs are series, parallel and series-parallel PHEVs. Nonetheless, the PHEVs have a charger connected to their battery pack, which enable the PHEVs to be recharged with energy from the distribution grid (Yong et al., 2015). PHEV's owner can choose between the electric and the internal combustion propulsion. To maximize the vehicle's efficiency, the electric motor can be chosen to propel the vehicle in short-distance travels and urban perimeters (Tie and Tan, 2013).

2.1.3 Battery electric vehicles (BEVs)

The BEVs are electric vehicles that are solely propel by an electric motor. Therefore, these EVs do not have an internal combustion engine. The battery pack of a BEV is recharged with energy from the grid distribution and from a kinetic energy recovery system. As it is an all-electric vehicle, a BEV is suitable for city-driving conditions (Yong et al., 2015).

2.2 Battery technologies

The most widely used device for energy storage in EVs is the battery and it is one of the main components of an EV (Tie and Tan, 2013).

Table 1 shows the main characteristics of the most common battery technologies used in BEVs and PHEVs.

	Specific energy (Wh/kg)	Life cycle	Energy efficiency (%)
Lead acid battery	35	1000	>80
Nickel battery			
Nickel-iron	50 - 60	2000	75
Nickel-zinc	75	300	76
Nickel-cadmium	50 - 80	2000	75
Nickel-metal hybrid	70 - 95	<3000	70
Lithium battery			
Lithium-iron sulphide	150	1000+	80
Lithium-iron phosphate	120	>2000	-
Lithium-iron polymer	130 - 225	>1200	-
Lithium-ion	118 - 250	2000	>95
Lithium-titanate	80 - 100	18000	-

Table 1: Main characteristics of the most commonly used battery technologies in BEVs and PHEVs.

Adapted from (Tie and Tan, 2013).

2.3 Chargers

The conditions in which the EVs recharge are extremely important in their impact on the adequacy of an electric system since these conditions reflect on how much power the EVs require from the grid distribution and on how long the EVs are connected to the grid (Yilmaz and Krein, 2013).

The charger is necessary because a direct current (DC) must recharge the battery pack and the grid distribution supplies energy with an alternating current (AC). Then, the charger is responsible for rectifying the grid AC current to a DC current suitable for recharging the battery pack (Yong et al., 2015).

The chargers are categorized into on-board and off-board with unidirectional or bidirectional power flow (Yilmaz and Krein, 2013).

The on-board chargers are located in the EVs and enable the battery pack to be recharged directly from any suitable power supply. However, these chargers have a limit power capacity due to restrictions in volume, weight and costs. Nowadays, most BEVs have a single-phase unidirectional on-board charger (Yilmaz and Krein, 2013).

On the other hand, the off-board chargers are less common and mostly used in specific charging stations for fast charging. The EVs may connect directly to the DC power output of the off-board charger. Nevertheless, as most EVs have an on-board charger, the off-board charger with a DC power output involves redundant power electronics and costs (Yilmaz and Krein, 2013).

Both on-board and off-board chargers can be unidirectional or bidirectional. A unidirectional charger only recharges the battery pack. On the other hand, a bidirectional charger can not only recharge the battery pack but also inject energy back to the grid (Yilmaz and Krein, 2013).

Currently, there are three levels of charging for EVs. Each one is described in table 2.

Power level types	Charger location	Typical use	Energy supply interface	Expected power level
Level 1 120 VAC (EUA) 230 VAC (EU)	On-board 1-phase	Charging at at home or office	Convenience outlet	1.4 kW (12 A) 1.9 kW (20 A)
Level 2 240 VAC (EUA) 400 VAC (EU)	On-board 1-phase or 3-phase	Charging at private or public outlets	Dedicated EV supply equipment	4 kW (17 A) 8 kW (32 A) 19.2 kW (80 A)
Level 3 208 - 600 VAC or VDC	Off-board 3-phase	Commercial, analogous to a filling station	Dedicated EV supply equipment	50 kW 80 kW

Table 2: Charging levels. Adapted from (Yong et al., 2015) and (Yilmaz and Krein, 2013).

According to Yilmaz and Krein (2013), the level 2 charging is the most widely spread charging type in private and public charging stations and, consequently, it is the most used charging type amongst EVs owners.

Table 3 shows the charging characteristics of some EVs under each charging level.

	Battery type and storage capacity	Level 1		Level 2		Level 3	
		Power	Charge time	Power	Charge time	Power	Charge time
Toyota Prius PHEV (2012)	Li-Ion 4.4 kWh	1.4 kW (120 V)	3 h	3.8 kW (240 V)	2.5 h	N/A	N/A
Chevrolet Volt PHEV	Li-Ion 16 kWh	0.96-1.4 kW	5 - 8 h	3.8 kW	2 - 3 h	N/A	N/A
Mitsubishi i-MiEV	Li-Ion 16 kWh	1.5 kW	7 h	3 kW	14 h	50 kW	30 min
Nissan Leaf	Li-Ion 24 kWh	1.8 kW	12 - 16 h	3.3 kW	6 - 8 h	50+ kW	15 - 30 min
Tesla Roadster EV	Li-Ion 53 kWh	1.8 kW	30+ h	9.6 - 16.8 kW	4 - 12 h	N/A	N/A

Table 3: Charging characteristics of some EVs. Adapted from (Yilmaz and Krein, 2013).

2.4 The electric vehicles' market

According to Duan et al. (2014), BYD F3DM was the first commercial PHEV and made its market debut in March 2010 in China. In the USA, the first plug-in EVs available in the market were the Chevrolet's Volt and the Nissan's Leaf later that year.

By the beginning of 2011, about 2.5 million EVs had been sold across the world. In the same period, the EVs reached a market share of 2% in the USA and 9% in Japan (IEA, 2011). The consulting firm PwC estimated the EV's market share in the USA in 2011 to be 1.7%, similar to the EV's overall market share in the world (PWC, 2012).

IEA (2011) estimates that by 2020 the BEVs and PHEVs sold worldwide each year will reach about 2.5 million and 5 million EVs, respectively.

In the regional markets subjected to the study of IEA (2011), there is also an estimate of steady and fast growth in the number of EV yearly sales. IEA (2011) studied the EV market in China, India and in the member countries of the Organisation for Economic Co-operation and Development (OECD).

IEA (2011) emphasizes that the estimates consider the effects of the 2008 financial crisis. Additionally, the agency also assumed that the countries would implement economic incentives to accelerate the EV integration.

To Kooroshy et al. (2016), the BEVs and PHEVs sales will reach 8 million vehicles yearly by 2025 in the world.

A more recent estimate by PwC for the number of BEVs manufactured yearly in Europe and the member countries of the European Free Trade Association (EFTA) is of 2,229,000 vehicles by 2021 (PWC, 2016).

Propfe et al. (2013) estimated that the number of EVs, including hybrids and BEVs, on German roads will reach 450,000 in 2020. This estimate is far behind the 1,000,000 EVs goal set by the German government for the same year (Trumper, 2013).

Hasset et al. (2011) predicted the number of EV sales in selected European countries for different scenarios of EV integration. The results are shown in table 4.

	Scenario 1			Scenario 2			Scenario 3		
	2020	2025	2030	2020	2025	2030	2020	2025	2030
Germany	127	253	495	262	613	889	541	1,207	1,666
UK	84	166	325	172	403	584	356	793	1,094
Spain	42	83	163	86	202	293	179	398	550
Portugal	7	15	29	15	36	52	31	70	97
Greece	10	21	41	22	50	73	45	99	137

Table 4: EV sales in selected European countries in thousands. Adapted from (Hasset et al., 2011).

Hasset et al. (2011) highlights that scenario 1 is the most likely to happen scenario. However, scenario 2 is the most appropriate for electric system planning and scenario 3 upper limit scenario.

Moreover, Hasset et al. (2011) estimated the number of EVs on Portuguese roads under the integration scenarios in 2020 and 2030.

	Scenario 1		Scenario 2		Scenario 3	
	EVs	(%)	EVs	(%)	EVs	(%)
BEV	36,480	20	115,662	30	362,904	48
PHEV	145,920	80	273,713	70	396,282	52
Total	182,400	100	389,375	100	759,186	100

Table 5: Number of EVs in Portugal for different scenarios of EV integration. Adapted from (Hasset et al., 2011).

2.5 State-of-the-art of the impact evaluation of EV integration into power systems

Giglioli et al. (2014) analysed the efficiency and adequacy of a system representing the Italian power system. The authors investigated the effects of different scenarios of EV integration and different charging strategies. The scenarios considered were low, 1.5 million EVs, and high, 15 million EVs. The energy consumed by the EV fleet each day were assumed 5.5 GWh and 55 GWh, respectively for the low and high integration scenarios.

The authors used a Sequential Monte Carlo simulation with time steps of 15min to analyse the different scenarios of EV integration and generate the adequacy indices.

The charging strategies considered by Giglioli et al. (2014) were daytime charging, charging during the night and mixed charging.

Liu et al. (2015) investigated the impact of PHEV integration into a Roy Billinton Test System (RBTS) with installed generation capacity of 240 MW and peak load of 185 MW. The authors used a Sequential Monte Carlo model to analyse the impact of the PHEVs.

The base scenario used by Liu et al. (2015) had 7,500 PHEVs. Of those PHEVs, 2,500 vehicles charged during the day while the rest charged during the night.

In order to evaluate the effect of an increase in the number of PHEVs on the adequacy of the system, the authors also considered a scenario of 15,000 PHEVs.

Moreover, Liu et al. (2015) also simulated a scenario with increased PHEV owners' willingness to have their PHEVs providing ancillary services, such as vehicle-to-grid (V2G), to the grid. This willingness was reflected by the total time for which the owners intended to provide auxiliary services through a charging control strategy.

Wang and Paranjape (2014) investigated the impact of EV penetration on the load curve of a 2,000 household distribution system under a direct charging strategy and the implementation of a Time-of-Use (TOU) demand response strategy.

Wang and Paranjape (2014) assumed three levels of EV penetration, 10%, 20% and 30%, which represented 200, 400 and 600 EVs, respectively, for the 2,000 household distribution system. Each scenario was evaluated under both the direct charging strategy and the TOU electricity price strategy.

Hemphill (2012) used data from the New South Wales Transport Data Centre (TCD), Australia, to estimate the load curve of PHEVs and BEVs in a substation zone.

In his study, Hemphill (2012) made the assumptions of linear discharging of the battery energy with the driving distance, charging with unit power factor and constant voltage and

current. For modelling the battery, the author used as base the Nissan Leaf's battery.

The author considered two levels of charging, 4 kW and 8.53 kW.

Hemphill (2012) based his estimate of the daily travelled distance on the data from TCD. The author used a lognormal distribution to sample the daily distance travelled by each EV. Hemphill (2012) considered that a fraction of the EVs would not respond to any charging control strategy. For this EV fraction, the author made the following assumptions:

- The EV starts recharging as soon as it arrives at home;
- Each EV recharges only once a day;
- The EV recharges until the SOC reaches 100%.

Hemphill (2012) estimated the number of recharging events every 5 min for a period of 24h.

In addition, Hemphill (2012) also investigated the use of what he called a smart control strategy. This strategy works under the following assumptions:

- EVs with the lowest SOC start charging first. The initial charging time of these EVs is linearly distributed between 22:00 and 06:00h.
- EVs with the highest SOC start charging first. These EVs start charging between 22:00 and 12:03 h for level 1 charging and between 22:00 and 3:44 h for level 2 charging. The EVs charging at level 1 charging are disconnected from the grid at 12:03h and those charging at level 2 charging are disconnected at 3:44h.

Soares et al. (2010) analysed the substitution of 25% and 50% of 2,285 light-weight cars for plug-in electric vehicles in the Flores Island, Portugal, in a typical winter day.

The authors noted that there was an increase of about 41% and 109% in the peak load and of 31% and 60% in the electricity consumption for the 24h period for the 25% and the 50% substitution levels, respectively.

Bremermann et al. (2014) used a Non-Homogeneous Poisson Process (NHPP) to evaluate the impact of EV integration on the generation adequacy. The results from the NHPP method were compared to a similar method based on the Homogeneous Poisson Process (HPP). The model presented by the authors uses real data from a Portuguese National Survey conducted by the Portuguese National Statics Institute. The authors investigated three charging strategies:

- Direct charging strategy (DC): the EV starts charging as soon as it ends the first trip of the day.

- Valley charging strategy (VC): the EVs may only start charging during the valley period.
- Controlled charging strategy (CC): the EVs may only charge during the valley period and, additionally, the suitable EVs can be temporally disconnected from the grid if the system adequacy is at risk.

The power system used by Bremermann et al. (2014) was a modified version of the IEEE RTS - 96 system called IEEE RTS - 96 HW. The IEEE RTS - 96 HW system had an installed generation capacity of 11,391.00 MW. Thermal power plants accounted for 8,965.00 MW of the total generation capacity, while wind farms had a share of 1,526.00 MW and hydro plants 900.00 MW. The system peak load was 8,550.00 MW.

The authors considered the following EV penetration scenarios:

- Low: 2.5% of the light-duty vehicles in 2030, 207,000 EVs;
- Moderate: 5.5%, 442,000 EVs;
- High: 11.0%, 863,000 PEVs. With a limit of 70% to the EVs that can be put under the controlled charging strategy.

Soares et al. (2011) considered 6,604 EVs, which accounted for a 52% integration. These EVs recharged under one of the following strategies:

- Dumb charging: the EVs may charge whenever they park at a residential zone with available power source;
- Dual Tariff Policy: under this strategy, 25% of the EVs recharge during the lowest electricity tariff period, between 23:00 and 8:00h, and the remaining still charge under the dumb charging strategy;
- Smart charging: an aggregator may temporally disconnect EVs if the system adequacy is jeopardized.

The authors noted a peak load increase of 85%, 96% and 11%, for the dumb charging strategy, the dual tariff policy and the smart charging strategy, respectively.

Shafiee et al. (2013) estimated the impact of PHEV integration in a 166 household load profile. The total number of vehicles, including ICE vehicles and EVs, was 352 vehicles. In their study, the authors evaluated the impact of the PHEVs integration in a sequence of years 2020, 2023, 2026 and 2050.

Qian et al. (2011) investigated the impact of EV integration on the power demand curve of the residential, commercial and industrial segments. The authors divided the EVs into private and corporate vehicles. The charging strategies considered in their study are the following:

- Uncontrolled domestic charging: there are no incentives to avoid charging during peak periods. The private vehicles recharge at an average of two times a day, while corporate vehicles start charging at 18h in weekdays;
- Uncontrolled off-peak domestic charging: the peak period starts at 7:00h and ends at 20:59h, the remaining of the day is off-peak. In this strategy, 50% of the private EVs and all corporate EVs start charging from 21:00h to 23:00h. The initial charging time for each EV is sampled from a uniform distribution;
- Smart domestic charging: a real time electricity price is applied and every EV starts charging at the moment of lowest energy price.

3 ASSESSMENT METHOD

The next subsections describe the assessment methods used in this study.

3.1 Long-term evaluation of generating systems

The planning of a generating system may be based on two different analysis, the security and the adequacy of the system. The later evaluates whether or not a future generating system will have sufficient generating capacity to meet the system demand whereas in the security analysis, the ability of the system to respond to disturbances arising from within the system is evaluated. Therefore, the adequacy analysis is associated with the static conditions of the generating system and the security is related to the dynamics of the system (Billinton and Allan, 1996).

The total generating capacity needed to ensure an adequate supply may be assessed through the evaluation of the static reserve and the operating reserve (Billinton and Allan, 1996).

3.1.1 Static reserve evaluation

The static reserve is defined as the difference between the system generating capacity and the load at a given time. Equation 1 gives the test function for the static evaluation (Bremmermann, 2014).

$$R_{static} = G - L_f \quad (1)$$

where G is the generating capacity and L_f is the load forecast. G depends on the availability of the equipment and on the fluctuations of hydrological and wind resources whereas L_f depends on the long and short-term uncertainties of the load forecast. If R_{static} is less than 0, then the system is in a failure state, otherwise, it is in a success state (Bremermann, 2014).

The risk indices used in the static reserve assessment are defined in Subsection 3.2.

3.1.2 Operating reserve evaluation

In the operating reserve evaluation, additionally to the previously mentioned parameters, the operation strategy and the reserve criteria are also taken into consideration (da Silva et al., 2010).

(Matos et al., 2009) defines operating reserve as the summation of the secondary reserve, spinning reserve, and the fast tertiary reserve, which is composed by units that can take up load within 1 hour.

The test function used to evaluate the power system in terms of operating reserve is given by Equation 2 (Matos et al., 2009).

$$R_{ope} = R_S + R_T - (\Delta L_f + \Delta W_S + \Delta G) < 0 \quad (2)$$

where R_S is the secondary reserve; R_T is the tertiary reserve; ΔL_f is the load forecast error; ΔW_S is the wind resource forecast error and ΔG represents the generating capacity variation due to forced outages.

If the inequality in Equation 2 is true, then the system is in a failure state.

Therefore, the operating reserve assessment evaluates not only the total generating capacity of an electric system, but also the flexibility of this system to cope with short-term uncertainties brought in by unpredicted load and generation variations (Bremermann, 2014).

Figure 4 summarizes the operating reserve concept.

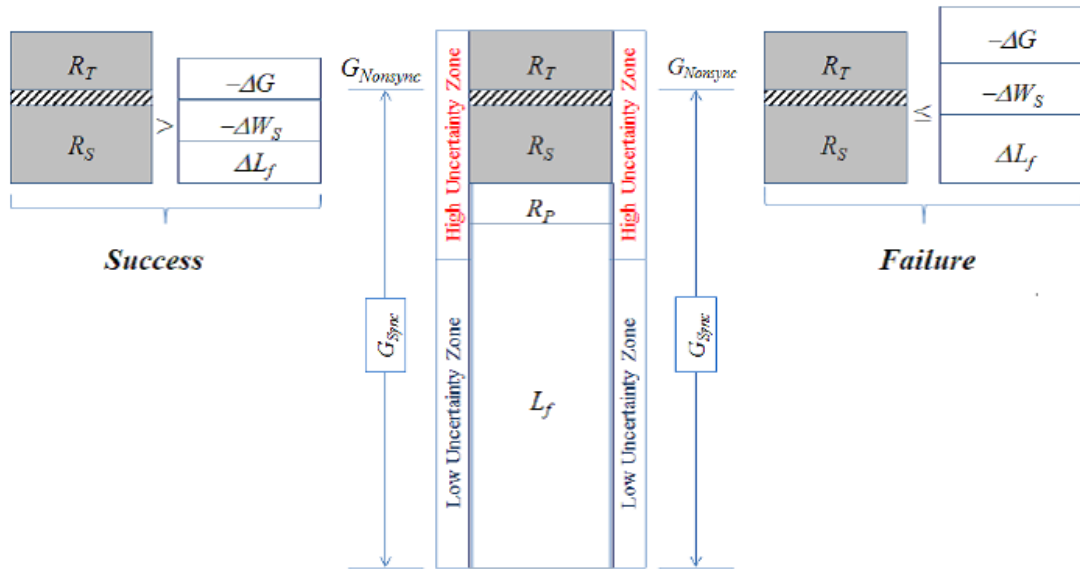


Figure 4: Operating reserve capacity evaluation (Bremermann, 2014).

Similar to the static reserve evaluation, the indices used to evaluate the operating reserve are defined in the next subsection.

3.2 Adequacy of supply

The adequacy of supply is defined as the availability of infrastructure and enough power to satisfy the consumer demand at a given time. Moreover, adequacy is considered to be associated with static conditions which do not include system disturbances (Billinton and Allan, 1996).

A power system may be divided into three hierarchical levels (HL). Each level can have its adequacy evaluated separately from the other two levels. The first level is composed by the generating units of the power system and it is called HLI. Level HLII refers to the composite generation and transmission system. Meanwhile, level HLIII includes not only the composite generation and transmission system but also the distribution system (Billinton and Allan, 1996). Figure 5 synthesizes this hierarchy.

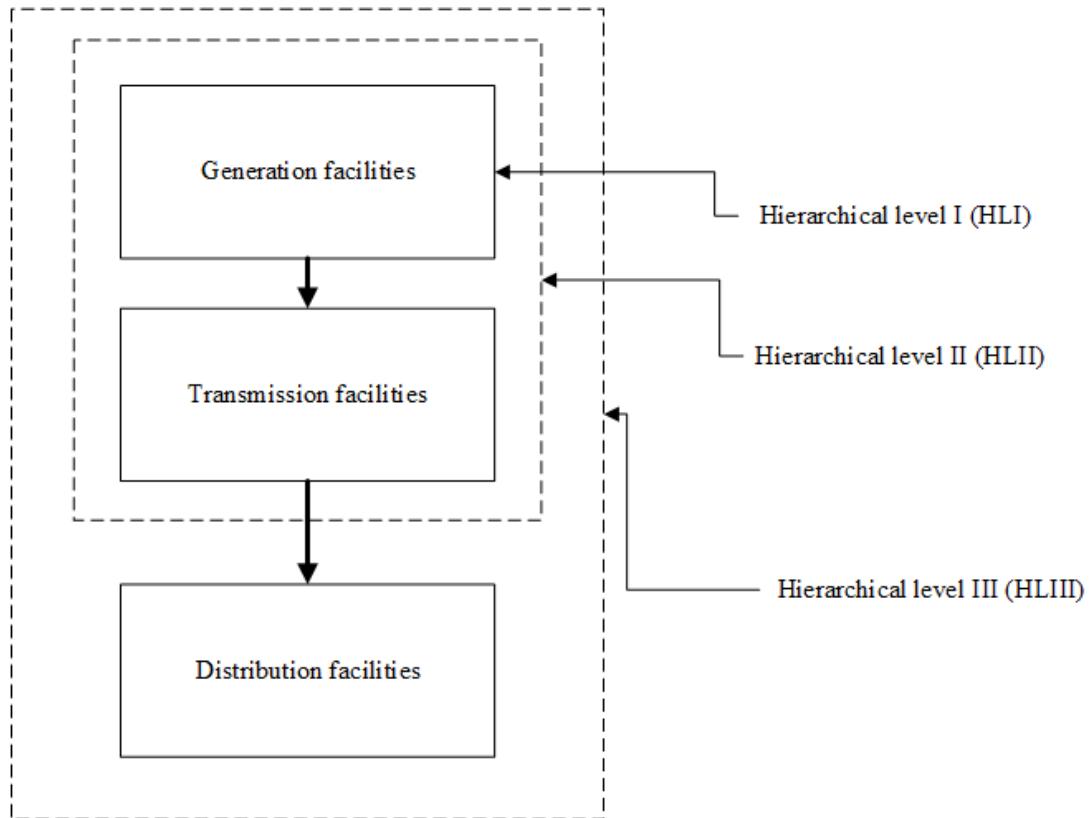


Figure 5: Hierarchical Levels. Adapted from (Billinton and Allan, 1996).

This study is concerned with the adequacy analysis of HLI.

Furthermore, in order to investigate the adequacy of supply of a system, a series of reliability indices is generally used. Those indices are categorized as probability, energy, frequency and duration indices (Billinton and Allan, 1996).

This study focuses on the adequacy of a generating system. The commonly used indices for this type of evaluation are defined by Billinton and Allan (1996) as:

- Loss of Load Expectation (LOLE): gives the expected mean time for which the system load is greater the system generating capacity. This index is usually given in hours/year or days/year;
- Expected Power Not Supplied (EPNS): expresses the mean expected power curtailed for a given period. It is given in MW;
- Expected Energy Not Supplied (EENS): gives the mean expected energy not supplied during the studied period. It is expressed in MWh/year;
- Loss of Load Frequency (LOLF): LOLF is the mean expected number of occurrences of load curtailment in occurrences/year or occurrences/month;

- Loss of Load Duration (LOLD): it is the mean expected duration of load curtailments in hours/occurrence.

The LOLE index can be calculated by Equation 3.

$$LOLE = \frac{1}{N_{year}} \sum_{u=1}^{N_{year}} \sum_{t=1}^{8760} F(u,t) \quad (3)$$

where N_{year} is the number of simulated years; t is the hour in year u and F is a binary variable that can assume the values 1 and 0. F is 1 if the system state in hour t of the simulated year u is a failure, i.e., if forecast load is greater than the available generating capacity, and 0 otherwise. The state duration was suppressed because the time step and the system state F duration are both equal to 1 h.

Similarly, EPNS may be expressed as:

$$EPNS = \frac{1}{8760} \frac{1}{N_{year}} \sum_{u=1}^{N_{year}} \sum_{t=1}^{8760} (L_f(u,t) - G(u,t))F(u,t) \quad (4)$$

where $L_f(u,t)$ is the forecast load and $G(u,t)$ is the available generating capacity. As in the LOLE equation, $F(u,t)$ will be 1 if $G(u,t)$ is not enough to meet demand $L_f(u,t)$ and 0 if there is sufficient generation capacity available.

The EENS can be obtained by modifying Equation 5 to yield:

$$EENS = \frac{1}{N_{year}} \sum_{u=1}^{N_{year}} \sum_{t=1}^{8760} (L_f(u,t) - G(u,t))F(u,t) \quad (5)$$

The LOLF index can be defined as:

$$LOLF = \frac{1}{N_{year}} \sum_{u=1}^{N_{year}} \sum_{t=1}^{8759} O_c(F(u,t+1) - F(u,t)) \quad (6)$$

where O_c is a binary variable that assumes 1 if $F(u,t+1) - F(u,t)$ is equal to 1 and 0 otherwise. That is, the failure occurrences are only accounted if they do not happen consecutively.

LOLD is then:

$$LOLD = \frac{LOLE}{LOLF} \quad (7)$$

The two main methods to analyse the adequacy of supply of a generating system are the analytical and the Monte Carlo approaches (Billinton and Allan, 1996).

3.2.1 Analytical method

In this approach, the system is represented by a set of mathematical equations that are numerically solved to generate the desired adequacy indices. This technique does not require

much computing time. Nevertheless, a series of assumptions must be made to simplify complex systems and operating procedures in order to enable a mathematical representation of them. Hence, the resulting analysis loses some or much of its significance (Billinton and Allan, 1996).

3.2.2 Monte Carlo method

The Monte Carlo methods, also called simulation methods or probabilistic methods, estimate the reliability indices by simulating the actual process and random behaviour of the system. These methods consider the repair and failure events of generating units, variations in the load, the dynamics of the hydro power generation units' reservoirs as well as all different types of operating policies. Hence, the Monte Carlo methods not only give the probability indices but also indices of frequency and duration of failures (Billinton and Allan, 1996).

The Monte Carlo method can follow one of the two approaches (Billinton and Allan, 1996):

- Non-Sequential: in this approach, basic intervals of time in the simulation period are simulated after randomly choosing these intervals. The non-sequential approach is also known as random.
- Sequential: this examines each basic interval of time of the simulated period in chronological order.

The choice of which Monte Carlo method approach to use depends on the characteristics of the system. Commonly, the non-sequential approach is used when the previous state of the system does not affect its present state. Alternatively, the sequential Monte Carlo method is preferred when the history of the system affects its present conditions (Billinton and Allan, 1996).

3.2.3 Non-sequential Monte Carlo method

In this method, the system state is randomly sampled regardless of the time interval period and the past states of the system. The system state is composed of each individual component state in the system. The state of the components is sampled from their respective probability distribution functions. After generating the system state, the test functions are calculated and the reliability indices are estimated (Rubinstein and Kroese, 2008).

The non-sequential Monte Carlo method may comprises the following steps (Rubinstein and Kroese, 2008):

1. Initialize the numbers of samples $N = 0$;
2. Sample the system state and update N ;
3. Calculate the test functions results for each reliability index;
4. Estimate each reliability index as the average of its test functions results calculated in step 3;
5. Calculate the coefficient of variation β . If the confidence degree is acceptable, then stop, if not, go to step 2.

3.2.4 Sequential Monte Carlo method

In the sequential Monte Carlo method, the state duration of each component is sampled from their respective state duration probability density function. Similar to the non-sequential method, the aggregation of all component states forms the system state (Rubinstein and Kroese, 2008).

The generating units of a power system can be represented by a two-state model. In this model, the generating unit is either in the operating state or in the repair state. The duration of both states are generally represented by an exponential distribution function (Rubinstein and Kroese, 2008).

For a sequential Monte Carlo method with a two-state component model and in which the time intervals are in hours and the maximum number of samples is defined in years, the simulation can be performed through the following steps (da Silva et al., 2005):

1. Sample the initial system state. Usually, in the initial system state, all components are operating. Define the maximum number of years, N_{max} , and the coefficient of variation, β . Set $N_{year} = 0$.
2. Initialize the number of hours $t = 0$ e update the number of years $N_{year} = N_{year} + 1$;
3. Update each component state at hour t .
4. Update t ;
5. Calculate and accumulate the test function results for each reliability index;
6. Update the reliability indices in a yearly basis;
7. If $t = 8760$, go to step 8, if not, go to step 4;
8. Update the reliability indices as the average of the yearly indices;

9. Check if the stop criteria have been reached;
10. If step 9 is false, go to step 2;
11. If step 9 is true, stop the simulation.

Figure 6 shows the steps described above in a flowchart manner.

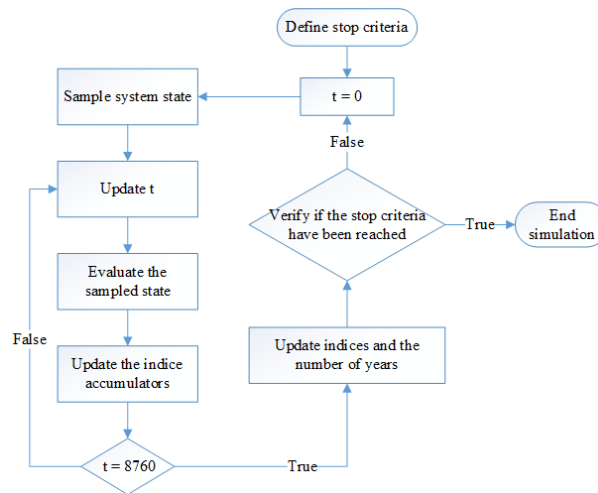


Figure 6: Sequential Monte Carlo method flowchart

3.3 The electric system

The electric system chosen for this study is a modified version of the IEEE Reliability Test System 1996 that accounts for the increasing presence of renewable energy in the generating systems. This modified version was created by (da Silva et al., 2010). The IEEE RTS - 96 is widely used in adequacy studies of electric systems.

It is important to highlight that in this study, the IEEE RTS - 96 is considered a single bus system.

(da Silva et al., 2010) named this as IEEE RTS - 96HW. It has an annual peak load of 8,550 MW and an installed capacity of 11,391 MW. The generating capacity is comprised by 900 MW of hydropower, 1,526 MW of wind power and 8,965 MW of thermal power units. Thus, renewable energy amounts for about 21% of the total installed capacity of the system.

Table 6 shows details of the generating units.

Group	Type	Cap. (MW)	No. of Units	Merit order	λ (occ./y)	MTTR (h)
U2	Wind	2.0	763	1	4.56250	80.0
U12	Oil	12.0	15	8	2.97959	60.0
U20	Oil	20.0	12	9	19.46667	50.0
U50	Hydro	50.00	18	10	4.42424	20.00
U76	Coal	76.0	12	5	4.46939	40.0
U100	Oil	100.0	9	7	7.30000	50.0
U155	Coal	155.0	480	4	9.12500	40.0
U197	Oil	197.0	600	6	9.22105	50.0
U350	Coal	350.0	2880	3	7.61739	100.0
U400	Nuclear	400.0	60	2	7.96364	150.0

Table 6: Characteristics of the generating units. Adapted from (da Silva et al., 2010)

In Table 6, λ is the failure rate and MTTR is the mean time to repair.

The merit order shown in Table 6 was based on the production cost. Due to the nature of its primary resource, the wind power generation has the highest priority in the dispatching. The hydro units are left at the final position of the list.

In this study, the primary and secondary reserve requirements of the electric system are set at 85 MW and 315 MW, respectively.

The wind and hydro series and further details of the electric system can be found in (da Silva et al., 2010).

With respect to the annual peak load, this system is similar in size to the Portuguese electric system (Nacionais, 2015). Figure 7 illustrates the seasonality of the electric system load used in this study.

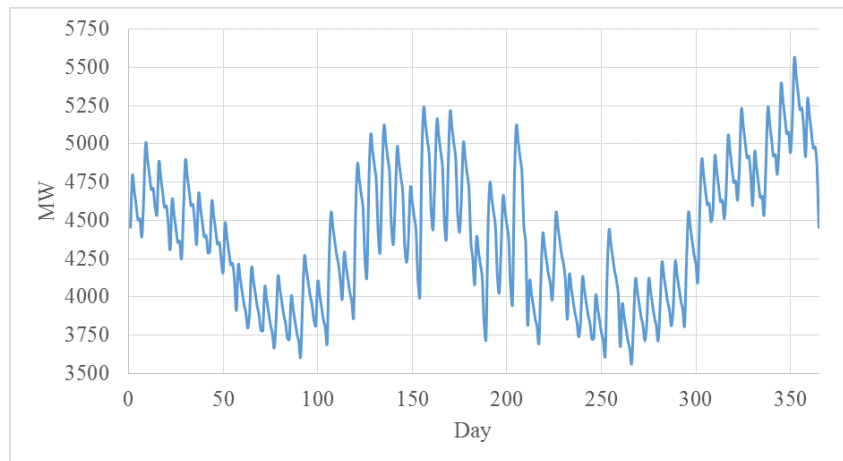


Figure 7: Electric system load profile

3.4 Demand side management

When the adequacy of an electric system is jeopardized at any of its levels, i.e, generation, transmission or distribution, the most traditional solution is to increase generation to meet the growing demand (Palensky and Dietrich, 2011).

However, Palensky and Dietrich (2011) highlights that grid capacity in electric systems is a source of concern and increases in generation and demand may cause the grid to reach its capacity limits soon. Additionally, electric systems face the challenging integration of renewable energy sources and electric mobility into their grids.

One way to cope with these new challenges is to use the load as an additional degree of freedom. This method is known as demand side management (DSM) and although it is not new, the improvements in communication infrastructure make it now possible to implement new solutions of DSM (Palensky and Dietrich, 2011).

DSM includes a series of actions made at the consumption side of the electric system. These actions can be changes in consumption patterns over short-term or long-term improvements in energy efficiency and optimizing allocation of power (Palensky and Dietrich, 2011).

Palensky and Dietrich (2011) categorizes DSM into the following:

- Energy Efficiency (EE): EE covers measures that promote permanent energy savings. Improvements in processes, exchanging inefficient equipment with efficient ones and improvements in physical properties, such as changes in building shell, are all considered EE measures;
- Time of Use (TOU): higher tariffs are applied to peak load periods and costumers rearrange their processes to minimize costs. TOU does not diminish energy consumption, instead it shifts consumption to periods of lower tariffs;
- Demand Response (DR): customers respond to a signal from the distribution or transmission system operator and reduce their power demand;
- Spinning Reserve (SR): SR is seen as primary control, when it acts to stabilize the system's frequency, and secondary control, when it aims to restore the frequency to an acceptable level. Loads can act as virtual SR if their active power consumption is related to the grid's frequency, i.e, when the frequency drops, the demand is automatically reduced.

DR can be further divided into the following types (Han and Piette, 2008):

- Direct load control: the system operator may shut down a load when a system contingency arises;

- Interruptible loads: costumers agree to reduce consumption when the system is at risk in exchange for lower tariffs;
- Emergency demand response: the system operators signalizes the need for load curtailment and costumers can decide whether or not to participate;
- Capacity market: customers commit to provide pre-specified load reduction when the system is jeopardized;
- Demand bidding: customers negotiate price and load curtailment in advance of a predicted system unbalance.

EVs can participate effectively in the DSM by offering ancillary services to the grid, such as load curtailment, change of its charging pattern and spinning reserve through the V2G technology (Antúnez et al., 2016; Liu et al., 2015).

3.5 Daily travelled distance

de Azevedo (2008) used data from vehicle inspections in Portugal to develop a method for estimating the national traffic volume. Among other results, de Azevedo (2008) synthesized the 2004 daily driven distance probability distribution of light-duty vehicles, which is shown in figure 8.

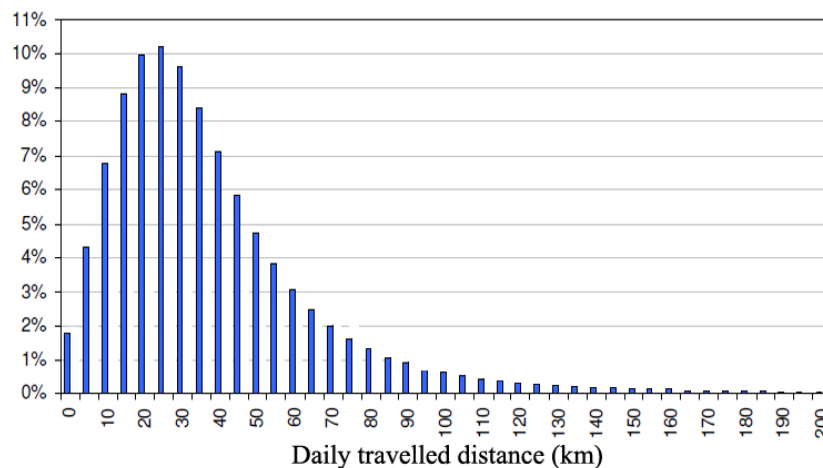


Figure 8: Daily travelled distance distribution. Adapted from (de Azevedo, 2008).

In this study, it is assumed that the mobility of the light-duty Portuguese vehicles has not changed since 2004. Furthermore, it is considered that, regardless the level of EV integration in Portugal, the driving behaviour of the Portuguese population will not change.

Then, in order to find a probability distribution function that reflects the Portuguese driving behaviour, the probability distribution curve found by de Azevedo (2008) is here approximated by a gamma probability distribution function. The MatLab distribution fitting tool was used to find the parameters of the gamma distribution function. The parameters found were a scale factor of 17.6404 and a shape factor of 2.2836, which give an average daily travelled distance of about 40 km.

Figure 9 shows the probability distribution curve used in this study.

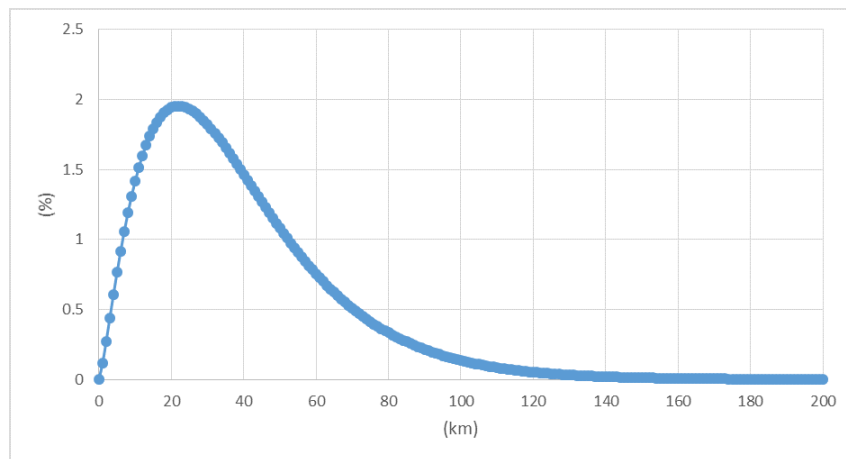


Figure 9: Probability density curve for the daily distance travelled by a light-duty vehicle in Portugal.

The probability density function is then used in the methodology explained in section 3.4 for sampling the daily travelled distance by each EV.

3.6 Home arrival and home departure times

The home arrival time for each EV is sampled on a daily basis time. The probability density functions of the home arrival and home departure times of light-duty vehicles used in this study are obtained from a national mobility pattern survey conducted by the Portuguese National Institute of Statistics. Figure 10 shows the probability distribution of the home arrival and departure time.

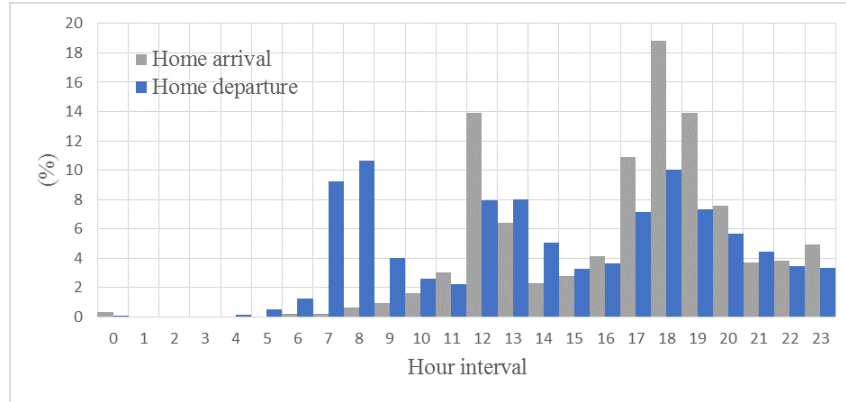


Figure 10: Home arrival time of light-duty vehicles in Portugal. Adapted from (de Estatística, 2002)

Table 7 gives the probability of each hour interval shown in figure 10. For instance, the probability of an EV home arrival be between 0:00:00 h and 0:59:59 h is 0.3% and so on.

Hour Interval	Arrival (%)	Depart. (%)	Hour Interval	Arrival (%)	Depart. (%)	Hour Interval	Arrival (%)	Depart. (%)
[0,1)	0.3	0.1	[8,9)	0.6	10.6	[16,17)	4.1	3.6
[1,2)	0.0	0.0	[9,10)	0.9	4.0	[17,18)	10.9	7.2
[2,3)	0.0	0.0	[10,11)	1.6	2.6	[18,19)	18.8	10.0
[3,4)	0.0	0.0	[11,12)	3	2.2	[19,20)	13.9	7.3
[4,5)	0.0	0.1	[12,13)	13.9	7.9	[20,21)	7.6	5.7
[5,6)	0.0	0.5	[13,14)	6.4	8.0	[21,22)	3.7	4.5
[6,7)	0.2	1.3	[14,15)	2.3	5.1	[22,23)	3.8	3.4
[7,8)	0.2	9.2	[15,16)	2.8	3.3	[23,0)	4.9	3.3

Table 7: Probability distribution of home arrival time and departure from home of light-duty vehicles in Portugal. Adapted from (de Estatística, 2002)

3.7 Sampling methodology

The methodology used in this study to sample values from the daily travelled distance, the home arrival and departure time probability distributions follows the steps described below.

1. Sample an abscissa value, x , using the uniformly distributed number generator developed by Bremermann (2014). For the daily travelled distance, x is in the range $[0, 200)$ and for the home arrival and the home departure time, that range is $[0, 24)$;
2. Sample an ordinate value, y , from the range $[0, 1)$;
3. Get the probability $g(x)$ from the probability distribution function;

4. Check if $g(x)$ is equal or less than y ;
5. If step 4 is true, define x as the distance travelled by the EV or as the home arrival or home departure time and go to step 7;
6. If step 4 is false, go back to step 1;
7. End of the sampling process.

3.8 EV modelling

As shown in Table 5, the EV fleet in Portugal will be formed by BEVs and PHEVs. Moreover, according to PWC (2016), the best selling PHEV and BEV in 2014 in Europe and the member countries of the European Free Trade Association were the Mitsubishi Outlander PHEV and the Nissan Leaf, respectively. Thus, a fleet formed by PHEVs similar to the Mitsubishi Outlander PHEV and BEVs similar to the Nissan Leaf is used in this study.

Thereby, a 12 kWh is assumed for all PHEVs. This choice is based on the battery size of the 2016 Mitsubishi 2.0 Hybrid GX4hs Automatic (Petrol) (Mitsubishi, 2016). Likewise, the 2016 NISSAN LEAF SV's 30 kWh battery is used for all BEVs (Nissan, 2016).

All EVs, BEVs and PHEVs, are assumed to have the same overall efficiency of 5 km/kWh, which is based on the average overall efficiencies of 30 kWh BEV models reported by IEA (2011).

The charging power for all EVs is assumed to be 4 kW, which is the power required by the charger from the grid (Yilmaz and Krein, 2013). The efficiency of the charger is set at 89.4% (Sears et al., 2014).

The batteries of all EVs are set to have a minimum SOC of 30% and a maximum SOC of 80%. Moreover, it is assumed that the power required by the battery during a charging event is constant.

A 759,815 EV fleet is considered in this study, which is the upper limit of the EV integration in Portugal, as it can be seen in table 5.

From now on, any mention of PHEVs and BEVs will refer to those with the characteristics described in this subsection.

3.9 Charging strategies

Four main charging strategies are used in the evaluation of EV integration into power systems. Each strategy is described below.

- Direct charging strategy: the EV will proceed to recharge disregarding the well-being of the electric system;
- Valley charging strategy: the EVs are allowed to recharge only during off-peak hours;
- Controlled charging strategy: in this strategy, the utility is able to postpone the recharging of suitable EVs as means of maintaining the balance between supply and demand. In this study, it is defined that an EV can have its recharging process postponed if its SOC is equal or greater than 70%;
- V2G charging strategy: under this strategy, the EV will be able to inject energy back to the grid when the electric system is at risk. Similar to the controlled charging strategy, an EV will inject energy back to the grid only if its SOC is equal or greater than 70%.

In this study, the direct, controlled and V2G strategy are used.

It is expected that not all EV owners will be willing to respond to a charging strategy at all moments and also that not all the households will have the infrastructure necessary to respond to those strategies, bearing this in mind, it is considered that only 20% of all EVs will respond to the controlled and V2G charging strategies.

3.10 Recharging criteria

Due to a lack of EV owners' recharging behaviour data, it is necessary to make assumptions about when an EV will start recharging.

In this study, three charging criteria are considered, namely, A, B and C.

In charging criterion A, the EVs will start recharging as soon as they arrive home.

In order to take into consideration the awareness of the EV owners about the fact that frequent recharging may cause a reduction in the battery's lifespan, charging criterion B is used. Under this assumption, the EV owner will start recharging their EV when it arrives home only if the present SOC is below 50%.

Furthermore, still bearing in mind the EV owner's awareness of the battery lifespan's reduction due to constant recharging and adding to it that the EV owner may only recharge

their EV enough to make the next day trip, recharging criterion C is considered. Under this assumption, the EV owner will start recharging their EV when it arrives home only if the present SOC is below the SOC necessary to make next day trip.

3.11 EV indices

To represent the EV behaviour, it is assumed that a EV could be in one of the three states: (1) discharging state, (2) charging state and (3) connected state. In state (1), the BEV is on the road and its battery pack is being depleted. In states (2) and (3), the EV is connected to the grid at home, but the EV is charging only when it is in state (2). In state (3), the EV is connected to the grid but it does not exchange energy with the grid.

The indices used in this study are the following:

- $N_{charging}$ index: gives the percentage of EVs in state (2) per hour in a period of 24 h as well as the standard deviation for each hour. The average number of EVs charging in hour h is given by Equation 8.

$$N_{EVs,charg}(h) = \frac{100}{N_{EVs}} \frac{1}{N_{days}} \sum_{n=0}^{N_{days}-1} N_{charg}(h+n24) \quad (8)$$

where N_{days} is equal to $N_{years}365$, $N_{charg}(h+n24)$ is the number of EVs charging in hour h and N_{EVs} is the number of EVs of the type under analysis. The standard deviation is then given by Equation 10.

$$A = \frac{1}{N_{days} - 1} \sum_{n=0}^{N_{days}-1} (N_{EVs,charg}(h) - N_{charg}(h+n24))^2 \quad (9)$$

$$Nstd_{EVs,charg}(h) = \frac{100}{N_{EVs}} \sqrt{A} \quad (10)$$

- $N_{connected}$ index: similar to the previous index, it gives the percentage and standard deviation of EVs in state (3) for each hour of a 24 h period. This index is calculated in an identical manner to the calculation of the previous index;
- N_{soc} index: the EVs in state (2) are divided in 20 groups according to their SOC. For example, the first group is comprised by the EVs in state (2) that have SOC equal or greater than 0% and are charging at a given hour. Likewise, the second group is formed by the EVs in state (2) that have SOC equal or greater than 5%. The subsequent groups

have a minimum SOC that increases by 5%. The mean number of EVs in each group is given for each hour of a 24 h period along with the standard deviation of the mean.

Equation 11 shows how the mean number of EVs charging during hour h that have a present SOC equal or greater than S is calculated.

$$Nsoc_{EV_s}[h, S] = \frac{100}{N_{EV_s}} \frac{1}{N_{days}} \sum_{n=0}^{N_{days}-1} N_{soc_{charg}}[h + n24, S] \quad (11)$$

when $N_{charg}[h + n24, S]$ is the number of EVs charging during hour h that have a present SOC equal or greater than S . Equation 13 gives the standard deviation of $N_{EV_s}[h, S]$.

$$V = \frac{1}{N_{days} - 1} \sum_{n=0}^{N_{days}-1} (Nsoc_{EV_s,charg}[h, S] - N_{soc_{charg}}[h, S])^2 \quad (12)$$

$$Nsoc, std_{EV_s,charg}[h, S] = \frac{100}{N_{EV_s}} \sqrt{V} \quad (13)$$

It is important to highlight that the indices created for this study are all given as percentage of the total number of the EV type under analysis. For example, say that $N_{charging}$ gives the average percentage of a given BEV type charging during hour h as $N_{EV_s,charg}(h)$ and the standard deviation for the same hour and EV type as $N_{std_{EV_s,charg}}(h)$. Thus, the average number of those BEVs charging during hour h is given by Equation 14 and the standard deviation is given by Equation 15.

$$BEV_{s,charg,avg} = \frac{1}{100} N_{EV_s,charg}(h) N_{BEV} \quad (14)$$

$$BEV_{s,charg,std} = \frac{1}{100} N_{std_{EV_s,charg}}(h) N_{BEV} \quad (15)$$

In both Equations, 14 and 15, N_{BEV} is the total number of the BEVs used in the analysis.

3.12 EV simulation

All simulations performed for this study were carried on a computer with the following specifications:

- Computer: HP ENVY m6;
- Operating system: Windows 10 Home;
- Processor: AMD A10-5750M APU with Radeon(tm) HD Graphics 2.50 GHz;
- Installed memory (RAM): 8.00 GB (7.46 GB usable);
- System type: 64-bit Operating System, x64-based processor.

The programming language chosen was Java and the platform used was Eclipse IDE, version Mars, release 4.5.0.

The methodology used for generating the indices described in Subsection 3.11 under charging criterion A is shown in Figure 11 for a single EV.

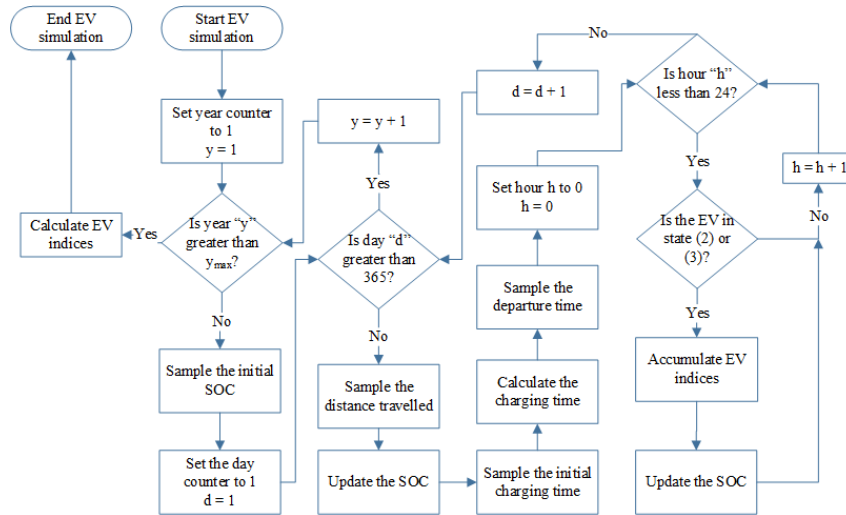


Figure 11: Flowchart of the EV simulation under charging criterion A

If the methodology shown in Figure 11 were to be applied to a few hundred thousands of EVs it would require an enormous amount of memory and take a considerable time to be executed. Hence, it is necessary to generate EV indices to reduce the computing effort needed to simulate the actual adequacy model of the EV integration into the electric system. These indices are generated separately for each charging criterion.

As presented in Figure 11, the EV indices are accumulated during every hour of the simulated years. When year y reaches $y_{max} + 1$, the averages and their standard deviations are finally calculated.

The EV simulation is performed in a chronological fashion. The initial charging time, i.e., home arrival time, happens always after the previous home departure time. Similarly, the home departure time always happens after the last hour that the EV is seen in states (2) or (3).

The stop criterion M_d used to determine the number of years necessary in the EV simulation is here the maximum deviation from the average. M_d is defined as the difference between the present average number of EVs charging during hour h and the previous average number of EVs charging during the same hour. This is possible because this average is calculated at the end of every simulated year.

M_d is calculated through Equations 16 and 17.

$$dev(h) = 100 \frac{N_{EVs,charg}(h)_y - N_{EVs,charg}(h)_{y-1}}{N_{EVs,charg}(h)_y} \quad (16)$$

where $N_{EVs,charg}(h)_y$ is the average number of EVs charging in hour h over y years and $N_{EVs,charg}(h)_{y-1}$ is the same average for $y-1$ years. h varies from 0 to 23 and $dev(h)$ is the deviation for hour h .

M_d is the maximum deviation, i.e., the maximum value of the vector dev .

$$M_d = \max([dev(h) : h = 0, 1, 2, \dots, 23]) \quad (17)$$

The stop criterion for M_d is set at 1% and the maximum number of years for this criterion be met is set at 10 years.

In this study, the indices described in Subsection 3.11 are generated using a fleet composed by 4,800 BEVs and 5,200 PHEVs. The characteristics of these two EV types are given in Subsection 3.8.

It is reasonable to assume that the energy demand of the BEVs and the PHEVs are independent variables. Thus, the EV indices are firstly calculated for the BEVs and subsequently for the PHEVs.

Figure 12 presents the indices $N_{charging}$ and $N_{connected}$ for the BEVs and PHEVs under charging criterion A.

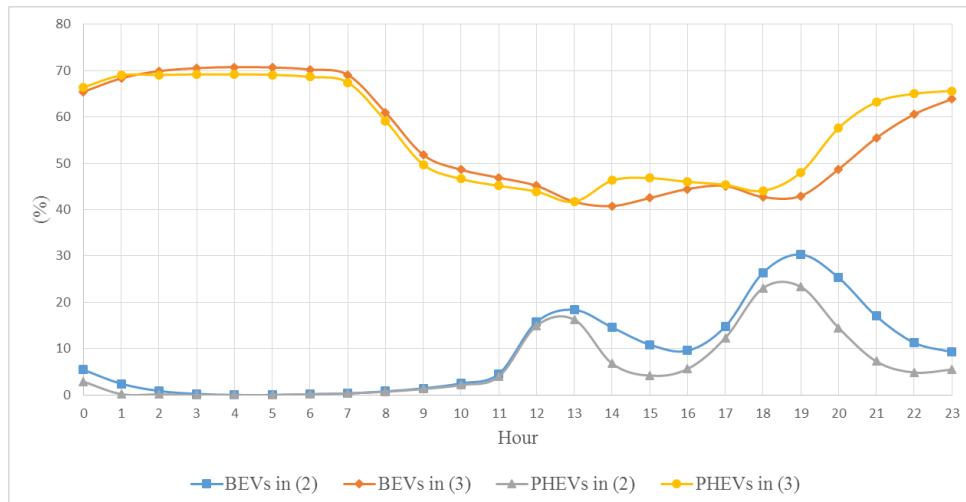


Figure 12: Percentage of BEVs and PHEVs in states (2) and (3) under charging criterion A for a 24 h period.

The indices can be used because the number of EVs charging during a given hour h can be approximated by a normal distribution, as Figure 13 shows for a 4,800 BEV fleet under charging criterion A and $h = 19$. The normal distribution in this figure has a mean of 1,454.86 and a variance of 2,133.44.

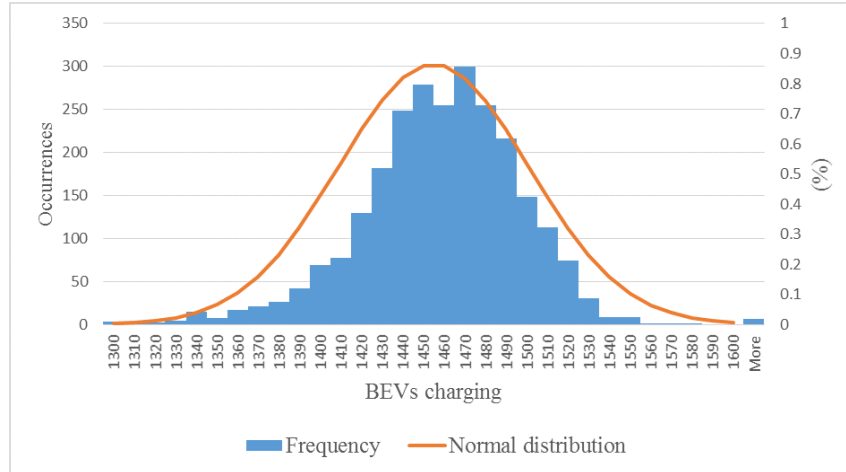


Figure 13: Distribution of the number of BEVs charging during hour 19 h under charging criterion A.

It is logical to assume that the number of EVs charging and connected will follow a normal distribution regardless the number or type of EVs, the hour or charging criterion chosen.

In order to evaluate the efficiency of using EV indices, a 10,000 EVs fleet and a 100,000 EVs fleet both composed by 48% BEVs and 52% PHEVs are used to estimate the EV demand under charging criterion A for both the methodology shown in Figure 11, traditional methodology, and using EV indices, proposed methodology. Tables 8 and 9 show these results.

(h)	Prop.		Trad.		Differences (%)	
	Mean (kW)	STD (kW)	Mean (kW)	STD (kW)	Dif_{mean}	Dif_{STD}
0	1642.7	135.6	1643.9	192.4	0.1	29.5
1	513.5	78.0	510.5	102.3	0.6	23.8
2	196.8	48.9	197.1	53.5	0.2	8.5
3	48.8	22.6	47.5	27.4	2.6	17.5
4	3.9	2.8	3.0	4.6	29.4	38.0
5	2.4	2.0	2.3	3.0	7.4	35.1
6	71.9	7.9	72.0	17.2	0.2	54.1
7	137.0	11.1	137.5	23.8	0.4	53.4
8	302.3	17.4	302.5	36.1	0.0	51.8
9	546.8	23.9	546.0	49.3	0.1	51.6
10	936.1	33.2	934.5	66.2	0.2	49.8
11	1703.9	51.5	1702.2	94.1	0.1	45.3
12	6,131.8	133.6	6,132.2	212.1	0.0	37.0
13	6,913.9	147.7	6,918.5	231.6	0.1	36.2
14	4,213.5	98.7	4,218.4	160.2	0.1	38.4
15	2,954.1	82.7	2,955.1	128.7	0.0	35.7
16	3,006.8	83.0	3,008.5	130.0	0.1	36.1
17	5,397.6	116.8	5,400.5	187.8	0.1	37.8
18	9,878.7	215.5	9,874.2	315.2	0.0	31.6
19	10,682.8	242.4	10,677.3	356.9	0.1	32.1
20	7,877.0	200.4	7,874.8	298.7	0.0	32.9
21	4,774.0	164.5	4,775.1	231.9	0.0	29.1
22	3,176.7	140.3	3,180.8	187.2	0.1	25.1
23	2,923.6	115.4	2,925.6	168.6	0.1	31.6

Table 8: Estimate of a 10,000 EV fleet demand under charging criterion A by the proposed and traditional methodologies

(h)	Prop.		Trad.		Differences (%)	
	Mean (kW)	STD (kW)	Mean (kW)	STD (kW)	Dif_{mean}	Dif_{STD}
0	16,422.3	1,308.1	16,433.2	1,764.5	0.1	25.9
1	5,129.0	763.4	5,104.4	932.5	0.5	18.1
2	1,969.1	467.5	1,972.3	460.6	0.2	1.5
3	485.2	223.3	474.4	238.8	2.3	6.5
4	39.1	24.1	30.3	31.9	29.1	24.5
5	22.7	4.7	22.8	9.8	0.3	52.1
6	718.6	38.1	720.3	61.2	0.2	37.7
7	1,370.9	57.7	1,372.8	91.1	0.1	36.6
8	3,021.4	98.3	3,020.6	147.9	0.0	33.5
9	5,460.9	147.9	5,458.2	223.1	0.0	33.7
10	9,344.7	232.2	9,346.2	334.0	0.0	30.5
11	17,021.3	400.4	17,022.8	545.8	0.0	26.6
12	61,323.0	1,243.9	61,322.8	1,632.1	0.0	23.8
13	69,163.0	1,369.7	69,182.1	1,823.3	0.0	24.9
14	42,188.6	860.2	42,185.5	1,118.1	0.0	23.1
15	29,552.9	715.9	29,554.0	836.4	0.0	14.4
16	30,081.6	710.9	30,084.0	821.2	0.0	13.4
17	54,001.4	1,029.4	54,008.0	1,358.9	0.0	24.3
18	98,732.3	2,020.1	98,757.4	2,690.5	0.0	24.9
19	106,801.7	2,345.6	106,792.6	3,155.4	0.0	25.7
20	78,791.0	1,925.7	78,764.8	2,590.9	0.0	25.7
21	47,776.3	1,595.3	47,757.4	1,982.8	0.0	19.5
22	31,822.8	1,337.1	31,798.5	1,593.6	0.1	16.1
23	29,243.7	1,067.5	29,245.1	1,374.4	0.0	22.3

Table 9: Estimate of a 100,000 EV fleet demand under charging criterion A by the proposed and traditional methodologies

The differences given in Tables 9 and 8 are calculated through Equation 18

$$D_f(h) = 100 \frac{P_n(h) - P_o(h)}{P_o(h)} \quad (18)$$

where $P_o(h)$ is the demand in h calculated through the steps shown in Figure 11 and $P_n(h)$ is the demand calculated using the EV indices.

It can be seen that the mean values of demand are practically not changed by the used of the proposed methodology. However, there is an average difference of about 30% between the standard deviation. This reduction in the standard deviation by the usage of the proposed methodology decreases the variability of the number of EVs charging, which, by consequence, may cause the adequacy simulation to fail to include extreme cases of EVs charging. Nevertheless, it is considered that this reduction in the standard deviation can be neglected in this study.

The main advantage of using the proposed methodology is the great reduction in computing time. Table 10 presents the average simulation time per simulated year for the proposed methodology and the traditional one. The results are given for EV fleets of 10,000, 25,000, 50,000, 75,000 and 100,000 EVs. The averages for the traditional approach were calculated

after simulating 100 years and for the proposed methodology the number of years was set at 103 years.

EVs (10^3)	Trad. (sec./year)	Prop. (sec./year)
10	12.14031	0.017336538
25	33.08854	0.015961538
50	60.91901	0.01775
75	90.1958	0.017759615
100	120.86944	0.01661165

Table 10: Estimate of a 100,000 EV fleet demand under charging criterion A by the proposed and traditional methodologies

A linear dependence of the simulation time per year on the number of EVs can be seen for the traditional approach. Based on the data given in Table 10, this linear dependence can be expressed by Equation 19.

$$S_{time} = 1.1916 * N_{EVs} + 1.4805 \quad (19)$$

where N_{EVs} is the number of EVs in thousands.

Using Equation 19 to estimate the average simulation time of a 759,186 EV fleet returns about 905 seconds per simulated year, which makes the usage of the traditional methodology impractical for purposes of adequacy assessment.

On the other hand, the estimate of the EV demand through EV indices is independent of the number of EVs because only the percentage of EVs charging is sampled during each simulated hour.

Nevertheless, the EV indices used in this study were generated using an EV fleet of 10,000. Which means that the estimate of, for instance, the 759,186 EV fleet was made based on the mobility and charging patterns of a 10,000 EV fleet. This is justified by the fact that the recharging events of an EV during any given time depends only on the daily driven distance distribution, the home arrival and departure times and the characteristics of the EV itself. Table 11 shows the demand of a 100,000 EV fleet based on EV indices generated by a 100,000 EV fleet and the demand of the same 100,000 EV fleet based on indices of a 10,000 EV fleet.

(h)	Based on a 100,000 EV fleet		Based on a 10,000 EV fleet		Differences (%)	
	Mean (kW)	STD (kW)	Mean (kW)	STD (kW)	D_{mean}	D_{STD}
0	16,422.3	1,308.1	16,426.7	1,356.1	0	4
1	5,129.0	763.4	5,134.6	780.2	0	2
2	1,969.1	467.5	1,967.9	489.1	0	5
3	485.2	223.3	487.8	226.0	1	1
4	39.1	24.1	39.5	24.7	1	3
5	22.7	4.7	23.6	11.1	4	136
6	718.6	38.1	718.6	77.1	0	102
7	1,370.9	57.7	1,369.6	109.7	0	90
8	3,021.4	98.3	3,023.3	173.3	0	76
9	5,460.9	147.9	5,467.8	238.3	0	61
10	9,344.7	232.2	9,361.3	331.7	0	43
11	17,021.3	400.4	17,039.4	514.1	0	28
12	61,323.0	1,243.9	61,317.9	1,336.2	0	7
13	69,163.0	1,369.7	69,139.0	1,476.7	0	8
14	42,188.6	860.2	42,135.0	986.7	0	15
15	29,552.9	715.9	29,540.8	827.0	0	16
16	30,081.6	710.9	30,067.6	830.3	0	17
17	54,001.4	1,029.4	53,976.6	1,167.6	0	13
18	98,732.3	2,020.1	98,786.6	2,154.8	0	7
19	106,801.7	2,345.6	106,828.0	2,423.7	0	3
20	78,791.0	1,925.7	78,770.4	2,003.9	0	4
21	47,776.3	1,595.3	47,740.5	1,645.4	0	3
22	31,822.8	1,337.1	31,766.8	1,402.8	0	5
23	29,243.7	1,067.5	29,236.1	1,153.5	0	8

Table 11: Comparison of the EV demand of a 100,000 EV fleet based on EV indices generated by different EV fleets

Once the indices have been generated, the EV integration into the electric system can be evaluated efficiently.

3.13 Adequacy evaluation

The adequacy evaluation was performed using a tool developed by Bremermann (2014).

The EV demand is sampled at the beginning of the simulated year. For doing so, firstly the number of EVs charging during hour h_{8760} is sampled through Equations 20 and 21.

$$h = h_{8760} - 24 \left(\max \left[n \in \mathbb{Z} \mid n \leq \frac{h_{8760}}{24} \right] \right) \quad (20)$$

$$EVs_{charging}(h_{8760}) = \max \left[n \in \mathbb{Z} \mid n \leq \frac{N_{EVs}}{100} \left[u * N_{std}_{EVs,charg}(h) + N_{EVs,charg}(h) \right] \right] \quad (21)$$

where u is a pseudo-random number that follows a normal distribution generated by the Box-Muller transform implemented by Bremermann (2014).

With the number of EVs charging, it is possible to calculate the EV demand using Equation 22.

$$Demand_{EV}(h_{8760}) = EVs_{charging}(h_{8760}) * P_{EV} \quad (22)$$

where P_{EV} is the charging power, 4 kW.

Once the EV demand is estimated, it is integrated to the conventional load profile. Then, the generating system capacity is sampled and the electric system state is evaluated on a hourly basis. Further information on the methodology used for generating the power system states and on the adequacy analysis can be found in (Bremermann, 2014).

4 RESULTS AND DISCUSSION

This section presents the results of the static and operating reserve evaluations in the analysis of a 759,815 EV fleet impact on the adequacy of the generating system described in Subsection 3.3. The characteristics of the EVs are given in Subsection 3.8, whereas the charging criteria and the charging strategies are given in 3.10 and 3.9, respectively.

Figure 14 presents the load profile of the 759,815 EV fleet.

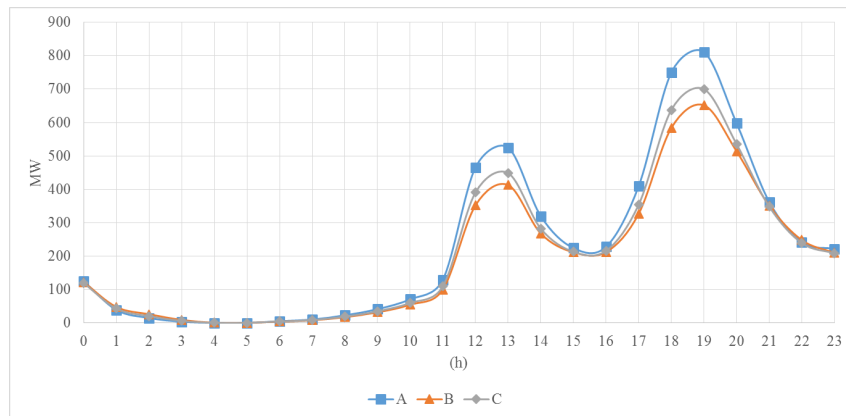


Figure 14: Load profile of the 759,815 EV fleet under different charging criteria.

The EV load profile matches the common drivers' behaviour, which is to arrive home around mid-day and early in the evening. The later is a source of concern for utilities and system operators because this behaviour can greatly increase the daily peak load.

Based on data from Figure 14, the daily energy consumption of the EV fleet under each charging criterion is given in Table 12.

Charging criterion	MWh/day
A	5,621
B	4,765
C	5,001

Table 12: EV fleet's daily energy consumption under each charging criterion

The impact of the direct charging strategy with charging criterion A on the load profile of a typical day is given by Figure 15.

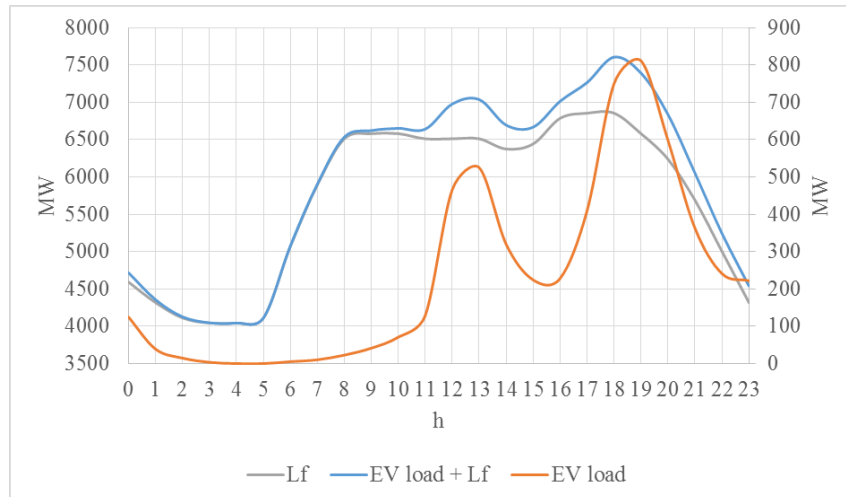


Figure 15: Impact of EV integration on the load profile of a typical day.

The load profile of a typical day sees a significant increase in the load during peak hours. However, the load in valley hours does not suffer a considerable change with respect to the load shape.

According to Pfeifenberger and Carden (2013), system operators commonly use the standard value of 2.4 h/year for the LOLE index when assessing the generating capacity of power systems. In addition to this standard LOLE, a base scenario (BS) with no EVs is used to compare the results obtained.

In order to ease the understanding, the following abbreviations will be used:

- DC&A: Direct Charging strategy takes place with charging criterion A
- DC&B: DC and charging criterion B
- DC&C: DC and charging criterion C

The results for the 759,815 EV fleet under the direct charging strategy and each charging criterion, along with the base scenario, are shown in Table 13.

Direct charging strategy								
	Static reserve evaluation				Operating reserve evaluation			
	BS	A	B	C	BS	A	B	C
Peak load (MW)	8,550	9,302	9,136	9,190	8,551	9,304	9,136	9,191
EV peak load (MW)	0	812	652	700	0	812	653	701
Peak load var. (%)	-	8.80	6.9	7.5	-	8.8	6.8	7.5
Mean load var. (%)	-	4.1	3.5	3.7	-	4.1	3.5	3.7
LOLE (h/year)	0.32	3.33	2.03	2.29	1.02	5.78	3.74	4.46
EPNS (MW)	0.01	0.09	0.05	0.06	0.03	0.24	0.14	0.17
EENS (MWh/year)	57.90	812.60	454.90	518.90	293.8	2,067.90	1,230.00	1,526.60
LOLF (occ./year)	0.12	1.90	1.08	1.25	0.41	2.97	1.84	2.22
LOLD (h/occ.)	2.74	1.76	1.88	1.82	2.49	1.95	2.04	2.01

Table 13: Static and operating reserve adequacy indices for the direct charging strategy under different charging criteria

The static reserve evaluation shows an increase of 8.8% in the peak load when DC&A is applied. However, if DC&B and DC&C are used, this increase is reduced to 6.9% and 7.5%, respectively. Similarly, when DC&A takes place, the mean increase in the system load is equal to 4.1%.

Moreover, the LOLE index is above the 2.4 h/year standard for DC&A and DC&C.

As it can be seen in Table 6, the wind units are at the first position of the dispatching list. Hence, the dispatch of generating units at all times must cope not only with variations in load forecast and outage of units but also with the uncertainty inherent to wind resource. At the operating stage, these uncertainties are dealt with by primary, secondary and tertiary reserves. Nevertheless, the static reserve evaluation fails to consider these reserve requirements. The importance of bearing in mind these operating contingencies when evaluating the adequacy of a generating system can be easily seen in the operating reserve analysis in Table 13.

The operating reserve evaluation shows a considerable growth in all risk indices when compared to the static reserve evaluation, except for the LOLD index. This reflects the importance of taking into consideration the operating policies and requirements of the electric system.

Since the short and long-term uncertainties of the load are set to 0, it was expected that the impact of EV integration on the load profile would be the same regardless if static or

operating reserve evaluation were used.

The results demonstrate a significantly lower impact on the adequacy of the generating system when charging criterion B is applied. This can be explained by the more restrictive nature of the charging criterion B when compare to A and C. Given the average daily driven distance of 40 km, the BEV consumes on average 27% of its battery capacity whereas for the PHEV this number is 67%. Thus, on average, the PHEV uses its entire SOC range available, i.e., SOC between the 30% minimum and the 80% maximum. Therefore, under charging criterion C, the BEVs will recharge, on average, only when their SOC is below 57% and the PHEVs will recharge as soon as they arrive home. On the other hand, under charging criterion B, both BEVs and PHEVs will recharge only if their SOC is below 50%. Hence, under charging criterion B, a charging event is less likely to happen.

The impact of EV integration on the adequacy of generating systems can be greatly reduced if EVs are regarded as capable of offering ancillary services to the grid. One of the most promising EV technologies is the V2G. However, the V2G has still to overcome a series of barriers. On the customers' side, V2G requires a bidirectional charger and relies on the willingness of the EV owner to provide ancillary services. On the utilities' end, there is the uncertainty of how much spinning reserve the V2G technology can account for and what will be its effect on the electric system security. Moreover, it is well established amongst researchers that the figure of an aggregator will be necessary to manage the ancillary services provided by EVs (Antúnez et al., 2016; Bremermann, 2014; Liu et al., 2015).

In other to account for the limiting factors in the spread of V2G technology, it is assumed that only 20% of the 759,815 EV fleet will be able to participate in the this strategy. Additionally, an EV will only send energy back to the grid and it is in state (3), i.e., connected to the grid, or when it is in state (2) with present SOC equal or greater than 70%. The power provided by each EV is considered to be 4 kW. This assumptions are applied for both BEVs and PHEVs.

In addition to the V2G technology, another option to reduce the impact of EV integration on power systems is the controlled charging strategy. In this strategy, the EV has its recharging postponed when there is no enough generating capacity available to meet the demand. In order to compare the controlled charging strategy to the V2G, it is assumed that only 20% of all EVs will participate in this strategy and that the recharging will only be postponed if the EV's present SOC is equal or greater than 70%.

The results for the static and operating reserve evaluations are given in Table 14 for the DC&A scenario under the V2G and the controlled charging strategies.

	Static reserve		Operating reserve	
	V2G	CC	V2G	CC
LOLE (h/year)	0.816728	2.56	2.64	5.71
EPNS (MW)	0.02	0.06	0.08	0.23
EENS (MWh/year)	177.5	562.6	673.6	1,990.1
LOLF (occ./year)	0.55	1.57	1.49	2.93
LOLD (h/occ.)	1.48	1.62	1.77	1.95

Table 14: Adequacy indices in the scenario of V2G and controlled charging (CC) implementations

It is promptly seen that, even if a small fraction of EVs participates in the V2G strategy, the impact of large-scale EV integration into the power system can be greatly reduced. The average energy provided by the V2G to the grid can be obtained by comparing EENS of Table 14 to that of Table 13. In the static reserve evaluation, the EVs sent back to the grid, on average, 635.1 MWh/year. In the operating reserve evaluation that number was 1,394.3 MWh/year. The LOLE index was also greatly reduced by the V2G implementation. In the static reserve analysis, this reduction was almost 75% whereas for the operating reserve it was more than 44%.

Despite the benefits of the V2G strategy, its availability is dependent on mobility and charging patterns. Therefore, the system operator must carefully account for this variability when dispatching the V2G as an additional spinning reserve.

The hourly V2G reserve follows a normal distribution and, for the reasons previously mentioned, the system operator cannot rely on the average V2G reserve. As an alternative, the operator can use the lower limit of a confidence interval of the V2G reserve as an additional spinning reserve. Figure 16 shows the average V2G reserve along with its lower limit of a 95% confidence interval in a 24 h period.

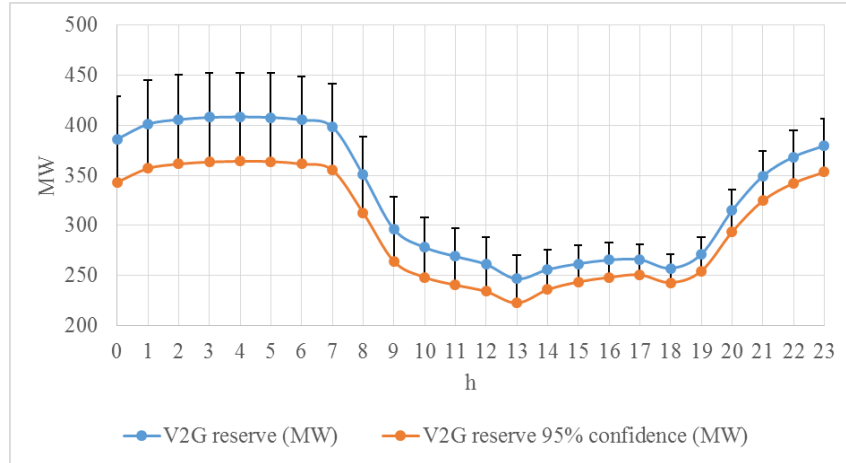


Figure 16: Impact of EV integration on the load profile of a typical day.

However, when the controlled charging strategy is applied to only 20% of the EV fleet, the impact of EV integration is slightly reduced. The LOLE index for the DC&A scenario under the direct charging strategy is reduced from 3.33 h/year to 2.56 h/year in the static reserve analysis, and from 5.78 h/year to 5.71 h/year in the operating reserve analysis. Similarly, the EENS index is reduced from 812.60 MWh/year to 562.6 MWh/year in the static reserve analysis and from 2,067.90 MWh/year to 1,990.1 MWh/year in the operating reserve analysis. This result shows that, in order to this technology to be effective, it needs massive participation of EV owners.

The usage of the sequential Monte Carlo simulation approach for solving generating system adequacy problems generally requires great computational effort and takes significant computing time. The addition of large-scale EV integration to the adequacy problem increases this burden. And, therefore, the EV integration requires a model that can reduce its computational effort requirements. Table 15 shows an estimate of the computing time that the traditional EV modeling approach would require to calculate the results given in Table 13.

	Direct charging strategy							
	Static reserve evaluation				Operating reserve evaluation			
	BS	A	B	C	BS	A	B	C
Number of simulated years	30,671	3,999	5,324	4,671	13,912	2,385	3,243	2,940
Computing time of prop. method (min.)	193.3	25.85	35.08	29.25	348.62	75.08	85.13	75.58
Computing time of trad. method (min.)	193.3	60,344.1	80,338.75	70,483.5	348.62	36,048.83	49,000.38	44,420.58

Table 15: Comparison of the computing time required by the traditional method and the proposed one

From table 15 it is also interesting to note that there is a sensitive decrease in the required number of simulated years when large-scale EV integration takes place. This can be explained by the reduction in the variability of the electric system states.

Due to the data used in this study, the EV demand tends to vary only during a day period. Moreover, Table 11 shows that the EV demand in a given hour does not vary significantly from one day to another. From Figure 14, it can also be seen that the 759,815 EV fleet represents a considerable load to the electric system. Therefore, the EV is a threatening load that has low variability.

Moreover, when V2G is not an option, the EV can only be a load to the electric system. Consequently, there is an increase in the number of possible failure states in any given hour and a decrease in the number of possible success states due to the additional EV load. As a result, the variance of the electric system state is reduced and the convergence of the adequacy indices happens more quickly.

On the other hand, when the EV can also send energy back to the grid, there is an growth in the variance of the electric system state and the computing time necessary to reach convergence increases. For instance, the results shown in Table 14 took 9,920 simulated years and 3,875 seconds to converge in the static reserve evaluation and 4,899 simulated years and 7,407 seconds in the operating reserve evaluation under the V2G strategy.

5 CONCLUSION

The methodology developed in this study for the evaluation of the impact of large-scale EV integration on the adequacy of generating systems shows satisfactory results with respect to both the computing performance and the expected results for the adequacy indices. It is shown that the proposed methodology reaches the same results as the traditional method, with losses only in the variance of the EV demand.

Furthermore, the results show that the criterion chosen by the EV owners to decide whether or not to recharge their EVs will have great importance in the impact of EV integration on power systems. Although is extremely unlikely that all EV owners will follow the same single criterion, the results of this study can be seen as ideal scenarios for the lower and upper limits of the EV impact on generating systems.

It is also shown that the V2G strategy can bring considerable benefits to the adequacy of generating systems even if only a small portion of the EV fleet is able to participate in the

the strategy. This is due to the fact that, in the V2G strategy, the EVs are able to act as micro-generators, contributing to the grid when an unbalance between load and generation arises.

On the other hand, when the controlled charging strategy is applied to only a fraction of the EV fleet, in this case, 20%, its benefits are far behind those of the V2G strategy. However, this is expected since the EV is regarded as just an interruptible load in the controlled charging strategy.

Additionally, the static and operating reserve evaluations are used to analyse each EV integration scenario and the importance of taking into consideration the operating parameters of the generating system is highlighted.

MODELO PARA AVALIAÇÃO DO IMPACTO DA INTEGRAÇÃO DE VEÍCULOS ELÉTRICOS EM SISTEMAS DE GERAÇÃO

RESUMO

Recentemente, a integração de veículos elétricos em sistemas de potência tem ganhado atenção substancial da academia e de empresas do setor elétrico principalmente por causa dos serviços auxiliares que essa tecnologia pode oferecer aos sistemas de potência. Ainda, a presença crescente de fontes renováveis nos sistemas de potência trouxe uma incerteza adicional à previsão de capacidade de geração disponível. Por isso, esse estudo tem como objetivo desenvolver um modelo de veículos elétricos para a avaliação do impacto da integração em larga escala de veículos elétricos na adequação de sistemas de geração. Para incluir a crescente presença de energia eólica, o método proposto é usado para avaliar o impacto da integração de veículos elétricos em uma versão modificada do sistema elétrico IEEE RTS-96. Os resultados mostram que o impacto da integração em larga escala de VEs na adequação de sistemas de geração depende do critério usado pelos proprietários dos VEs no momento de decidir por carregar ou não seus VEs. Ainda, é mostrado que o impacto dos VEs pode ser reduzido e até mesmo ser positivo, se os VEs são considerados provedores de serviços auxiliares à rede.

Palavras-chave: Adequação. Veículo elétrico. Sistema de geração. Sistemas de potência.

REFERENCES

- Antúnez, C. S., Franco, J. F., Rider, M. J., and Romero, R. (2016). A new methodology for the optimal charging coordination of electric vehicles considering vehicle-to-grid technology. *IEEE Transactions on Sustainable Energy*, 7(9):596–607.
- Billinton, R. and Allan, R. N. (1996). *Reliability Evaluation of Power Systems*.
- Bremermann, L. E. (2014). Impact evaluation of the large scale integration of electric vehicles in the security of supply.
- Bremermann, L. E., Matosa, M., Lopes, J. A. P., and Rosa, M. (2014). Electric vehicle models for evaluating the security of supply. *Electric Power Systems Research*, 111:32–39.
- da Silva, A. L., Sales, W., Manso, L., , and Billinton, R. (2010). Long-term probabilistic evaluation of operating reserve requirements with renewable sources. *IEEE Trans. Powers Systems*, 25(1):106–116.
- da Silva, A. M. L., Schmitt, W. F., Cassula, A. M., and Sacramento, C. E. (2005). Analytical and monte carlo approaches to evaluate probability distributions of interruption duration. *IEEE Trans. Power Syst.*, 20(3):1341–1348.
- de Azevedo, C. M. L. (2008). Métodos de estimativa de volumes anuais de tráfego rodoviário: Um modelo para portugal.
- de Estatística, I. N. (2002). Inquerito a mobilidade da população residente 2000.
- Duan, Z., Gutierrez, B., and Wang, L. (2014). Forecasting plug-in electric vehicle sales and the diurnal recharging load curve. *IEEE Trans. Smart Grid*, 5(1):527–535.
- Giglioli, R., Giuntoli, M., Lutzemberger, G., and Poli, D. (2014). Impact of a large fleet of evs on the efficiency and reliability of an electric power system. In IEEE, editor, *2014 IEEE International Electric Vehicle Conference*.
- Han, J. and Piette, M. (2008). Solutions for summer electric power shortages: Demand response and its applications in air conditioning and refrigerating systems. *Refrigeration, Air Conditioning, & Electric Power Machinery*, 29(1):1—4.

- Hasset, B., Bower, E., , and Alexander, M. (2011). Deliverable 3.2 ev penetration scenarios.
- Hemphill, M. (2012). Electricity distribution system planning for an increasing penetration of plug-in electric vehicles in new south wales. In IEEE, editor, *Universities Power Engineering Conference*.
- IEA (2011). Technology roadmap: Electric and plug-in hybrid electric vehicles.
- Kooroshy, J., Ibbotson, A., Lee, B., Bingham, D. R., and Simons, W. (2016). The low carbon economy: Gs sustain equity investor’s guide to a low carbon world.
- Liu, Z., Wang, D., Jia, H., Djilali, N., and Zhang, W. (2015). Aggregation and bidirectional charging power control of plug-in hybrid electric vehicles: Generation system adequacy analysis. *IEEE Trans. Sustain. Energy*, 6(2):325–335.
- Matos, M., Lopes, J. P., Rosa, M., Ferreira, R., da Silva, A. L., Sales, W., Resende, L., Manso, L., Cabral, P., Ferreira, M., Martins, N., Artaiz, C., Soto, F., and López, R. (2009). Probabilistic evaluation of reserve requirements of generating systems with renewable power sources: The portuguese and spanish cases. *Electrical Power and Energy Systems*, 31(9):562—569.
- Mitsubishi (2016). Mitsubishi vehicle comparison.
- Nacionais, R. E. (2015). Relatório & contas 2015.
- Nissan (2016). Interactive brochures.
- Palensky, P. and Dietrich, D. (2011). Demand side management: Demand response, intelligent energy systems, and smart loads. *IEEE Transactions on Industrial Informatics*, 7(3):381–388.
- Pfeifenberger, J. P. and Carden, K. (2013). Resource adequacy requirements: Reliability and economic implications.
- Propfe, B., Kreyenbergb, D., Windb, J., and Schmida, S. (2013). Market penetration analysis of electric vehicles in the german passenger car market towards 2030.
- PWC (2012). Charging forward: Pwc’s 2012 electric vehicle survey.
- PWC (2016). Europe: Electrification and beyond: A market outlook on emissions and electric mobility.

- Qian, K., Zhou, C., Allan, M., and Yuan, Y. (2011). Modeling of load demand due to ev battery charging in distribution systems. *IEEE Trans. Power Syst.*, 26(2):802–810.
- Rubinstein, R. Y. and Kroese, D. P. (2008). *SIMULATION AND THE MONTE CARLO METHOD*.
- Sears, J., Roberts, D., and Glitman, K. (2014). A comparison of electric vehicle level 1 and level 2 charging efficiency. In IEEE, editor, *Technologies for Sustainability (SusTech), 2014 IEEE Conference on*.
- Shafiee, S., Fotuhi-Firuzabad, M., and Rastegar, M. (2013). Investigating the impacts of plug-in hybrid electric vehicles on power distribution systems. *IEEE Trans. Smart Grid*, 4(3):1351–1360.
- Soares, F. J., Lopes, J. A. P., and Almeida, P. M. R. (2010). A monte carlo method to evaluate electric vehicles impacts in distribution networks. In IEEE, editor, *2010 IEEE Conference On Innovative Technologies For An Efficient And Reliable Electricity Supply*.
- Soares, F. J., Lopes, J. A. P., and Almeida, P. M. R. (2011). Integration of electric vehicles in the electric power system. *Proceedings Of The IEEE*, 99(1):168–183.
- Tie, S. F. and Tan, C. W. (2013). A review of energy sources and energy management system in electric vehicles. *Renewable And Sustainable Energy Reviews*, 20:82–102.
- Trumper, S. C. (2013). Commercial fleets as early markets for electric vehicles. In IEEE, editor, *16th International IEEE Conference On Intelligent Transportation Systems*.
- Wang, Z. and Paranjape, R. (2014). An evaluation of electric vehicle penetration under demand response in a multi-agent based simulation. In IEEE, editor, *2014 IEEE Electrical Power And Energy Conference*.
- Yilmaz, M. and Krein, P. T. (2013). Review of battery charger topologies, charging power levels, and infrastructure for plug-in electric and hybrid vehicles. *IEEE Transactions On Power Electronics*, 28(5):2151–2169.
- Yong, J. Y., Ramachandaramurthya, V. K., Tana, K. M., and Mithulananthan, N. (2015). A review on the state-of-the-art technologies of electric vehicle, its impacts and prospects. *Renewable And Sustainable Energy Reviews*, 49:365–385.

ACKNOWLEDGMENTS

The author thanks Prof. Leonardo Bremermann for the advices, support and patience throughout this study; INESC P&D Brasil for the undergraduate research scholarship and UFSC for the access to IEEE and ScienceDirect digital libraries.